Monitoring the Norwegian Atlantic slope current using a single moored current meter

Kjell Arild Orvik [a] and Øystein Skagseth[a, b]

[a] Geophysical Institute, University of Bergen, Allegaten 70, N-5007, Bergen, Norway
[b] Bjerknes Centre for Climate Research, University of Bergen, Allegaten 70, N-5007, Bergen, Norway

Abstract

Monitoring the Atlantic inflow (AI) of warm and saline water into the Nordic Seas (Norwegian, Greenland and Iceland Seas) is of great importance becauce of its impact on climate and ecology in Northern Europe and Arctic. In this study, an observation system for establishment of simple, robust and cost effective monitoring of the AI is validated in the Svinøy section, cutting through the AI just to the north of the Faroe-Shetland Channel. We concentrate on the eastern branch of the AI, the Norwegian Atlantic Slope Current (NwASC), an about 40 km wide flow along the steep Norwegian slope. The database is an array of 15 current meters on 4 moorings covering the NwASC over a 2-year period 1998–2000. We test the hypothesis that long-term monitoring of the NwASC can be performed by using one single current meter suitable placed in the flow. The volume flux can then be estimated by construction of simple regression models using the single current meter record as the independent variable. For validation of statistical properties as stability, confidence and stationarity, the time series is split into two 1-year segments: a model period and a test period. Gridded correlation fields between currents and volume transport show correlation maxima in the core of the NwASC, ranging from 0.84 on a daily timescale to 0.97 on a monthly timescale. A more comprehensive correlation/coherence analysis for each current meter record against volume transport on 7-day timescales, enable us to choose the optimal current meter for a linear regression model with (correlation, slope) coefficients of (0.87, 0.13) for the model period and (0.80, 0.13) for the test period. The similarity of the statistical properties for the model and test periods substantiates the stationarity, stability and robustness of the model. A linear regression model underestimates large fluxes and is thus extended to a second degree polynomia. This improves the curve fitting for strong currents with a minor increase in overall correlation, but is more sensistive and less stable. Overall, we find a linear regression model to be more robust and applicable for monitoring the NwASC. The applicability of a linear regression model as an estimator for volume flux of the NwASC is demonstrated using a 2-year time series, and validated against calculated transport. The calculated transport agrees with the statistical analysis and reveals a noisy fit on daily timescale, while the curves coincide well on both 7- and 30-day timescales with correlation coefficients of 0.84 and 0.86, respectively. On all timescales, the calculated and model transport give an overall mean flow of 4.4 Sv and show fluctuations on timescales of days to months, with the seasonal cycle being the most prominent.

Author Keywords: Atlantic inflow; Norwegian atlantic slope current; Volume transport; Moored current records; Monitoring; Linear regression model

1. Introduction

The Atlantic inflow (AI) of warm and saline water into the Nordic Seas (Norwegian, Greenland and Iceland Seas), and its extension northward to higher latitudes, is an important factor for climate and biological production in Northern Europe and Arctic. From a global warming perspective it has been suggested that an increase in the concentration of greenhouse gases in the atmosphere will disrupt this inflow (Wood et al., 1999; Rahmstorf, 1999). Since the consequences of a disruption of this AI may cause dramatic climatic changes for Northern Europe and the Arctic, a reliable system for monitoring volume, salt and temperature fluxes is of great importance. In this study, an observation system for the establishment of simple, robust and cost effective monitoring of major parts of the AI will be validated. The main basis for the study is a series long-term observations in the Svinøy section, which have been made since 1995 (Orvik et al., 2001). The Svinøy section runs northwestwards from the Norwegian coast at 62°N, and cuts through the AI just to the north of the Faroe-Shetland Channel (Fig. 1).

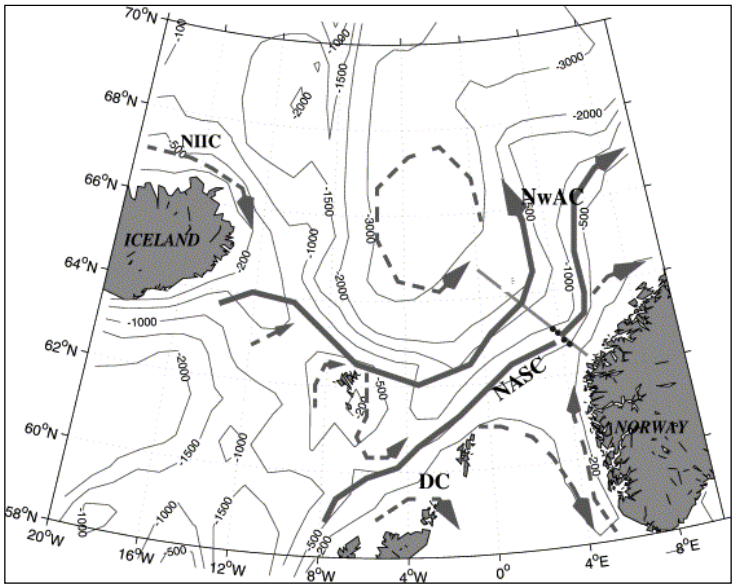

Fig. 1. Map of the study area, schematics of currents, Svinøy section, mooring locations (&z.cirf;). Solid lines outline the major currents and dashed lines indicate other currents. Contour lines show bathymetry (*m*).

In a historical perspective, the Norwegian Atlantic Current (NwAC) has been considered as a warm, saline, wedge-shaped current about 300 km wide, extending from the Norwegian shelf into the Norwegian Sea. Volume flux estimates range from 2.0 Sv (1 Sv=10^6 m^3 s^{-1}) (Tait, 1957; Mosby, 1970) to 9 Sv (Worthington, 1970). Poulain et al. (1996) showed a two-branch structure of the NwAC in the southern Norwegian Sea, using near-surface Lagrangian drifter observations, and referred to them as the western and the eastern branch of the NwAC (Fig. 1). Orvik et al. (2001) identified these two branches as an eastern branch which acts as a 30–50 km wide, shelf edge current, denoted the Norwegian Atlantic Slope Current (NwASC); and a western branch which is a 30–50 km wide, topographically steered jet in the Polar Front (the transition zone between the Atlantic and Arctic water in the Nordic Seas). Transport estimates from current records in the eastern branch show an annual mean AI of 4.2 Sv, while the mean baroclinic transport west of the eastern branch, including the frontal jet, was 3.4 Sv (Orvik et al., 2001). In a recent paper, Orvik and Niiler (2002) show from near-surface Lagrangian drifter observations that the NwAC appears to maintain its two-branch structure throughout the Nordic Seas toward the Fram Strait, with the Atlantic water confined to a 200–600 km wide wedge between the branches.

Concerning monitoring, Pistek and Johnson (1992) and Samuel et al. (1994) have shown examples of AI monitoring using satellite altimetry. McClimans et al. (1999) suggested an algorithm for monitoring the AI by using coastal sea-level observations, based on the conjecture of a fixed ratio between the fluxes in the barotropic and baroclinic parts of the NwAC.

The Svinøy section observation program includes an array of long-term current measurements of the NwASC in combination with VM-ADCP/SeaSoar-CTD transects, and it is well placed to undertake a comprehensive study of the Atlantic inflow with respect to transport estimates and structure. This also makes the Svinøy section applicable as a key area for monitoring the AI. In this study, we will concentrate on the establishment of a monitoring system for the NwASC by evaluating a simple and cost effective system consisting of one moored current meter. We will concentrate on the NwASC, primarily because of its data coverage, but also because the eastern and western branches of the NwAC may affect the Nordic Seas and Arctic differently. The western branch through the Nordic Seas will tend to feed the interior of the Nordic Seas, whereas the eastern branch (NwASC) will favor fluxes into the Barents Sea and the Arctic (Orvik and Niiler, 2002). In fact such arguments provide a link to the recent reduction of the Arctic ice cover (Johannessen et al., 1999; Rothrock et al., 1999), and substantiate the importance of monitoring the NwASC.

The structure of the NwASC in the Svinøy section has been analysed recently by Skagseth and Orvik (2002) using empirical orthogonal functions (EOF), and also by Orvik et al. (2001). These studies showed that the annual mean current is a stable flow about 40 km wide, along the isobaths over the steepest slope between the depths of 200 and 900 m. The strongest currents are located between 200 and 700 m depth, and their annual mean is 30 cm/s. The core of the mean flow shows a uniform velocity profile vertically, while there is a vertical velocity shear on the deeper side of the current. For the 1-year period April 1997–March 1998, the fluctuations of the NwASC are a combination of longer periodic forced oscillations which are a direct response to the wind, and free waves corresponding to the first and second topographic wave modes. The

direct response to the wind appears as an along-slope current with prominent periods in the 3–5 day and 16–32 day bands, with a structure similar to the mean flow. The free oscillations identified as first and second topographic wave modes, have dominant periods of 40–70 and 80–110 h, respectively.

In the above perspective, a monitoring system of the NwASC based on one moored current meter will be validated. In Orvik et al. (2001) it was shown that on a monthly timescale, the core of the NwASC was stable over the steep slope for the 2-year period October 1996–October 1998. It was also demonstrated that the volume flux of the NwASC could be represented reasonably well by using a single current meter record. This forms the basis of a hypothesis that long-term monitoring of the volume flux of the NwASC can be performed by using simple regression models based on records from a single current meter, suitably placed in the flow.

Consequently, in this study a more comprehensive analysis will be performed, to show connections between each current meter record in an array over the slope intercepting the NwASC, and the associated transport of Atlantic water (AW). The current records span a 2-year period from April 1998 to April 2000. In order to validate statistical properties as confidence, stability and stationarity, the time series will be split into two 1-year segments; a model period and a test period. Similar procedures will be performed for all cases by (1) establishing a model based on the model period and (2) testing the model's applicability against the test period. The main points for validation and selection of optimal current meter location for application, will be as follows: (1) Correlation/coherence analyses between volume transport and current records in an array over the slope. (2) Construction of linear regression models of volume flux for each current meter record. (3) An optimal current meter record location will then be selected from a thorough analysis, including construction of regression lines, for both the linear and the non-linear model. (3) Further, the applicability of a simple linear regression model will be demonstrated using a 2-year model time series of volume transport, and then validated against the volume transport computed from the array of 15 current meter records.

2. Data and analysis method

The study is based on moored current measurements in the Svinøy section for the 2-year period from April 1998 to April 2000. Table 1 gives an overview of current meter records for (a) the model period 1998–1999 and (b) the test period 1999–2000; including mooring positions, bottom depth and instrument depth, review of data recovery and statistics for each current meter record. The four mooring sites are indicated in Fig. 1, and the moorings and depths of the associated 15 recording current meters (RCM) are indicated in the hydrographic regime in Fig. 2. Fig. 2 also outlines the profile of the bottom topography along the section. The RCMs sample hourly, and were deployed and recovered at approximately 6-month service intervals. The spacing between the easternmost and westernmost moorings is about 46 km and the distance between adjacent moorings is about 15 km. The hydrographic regime is characterized by the wedge-shaped warm and saline Atlantic Water (AW) restricted to the water mass with salinity S>35.0 (Helland-Hansen and Nansen, 1909), corresponding to temperature T>5°C (Orvik et al., 2001), overlying the fresher and colder Norwegian Sea Deep Water. The interface between these water masses meets the bottom slope at about 600 m depth

Table 1. Data overview of current meter measurements and current statistics of the NwASC

Morning	Position	Depth (m)		Ext. of rec.	Mean velocity		Kinetic energy		Temperature	
		Water	RCM	Time (days)	Magnitude, (cm s^{-1})	Direction (deg,)	Mean (g cm^{-1} s^{-2})	Fluctuations, (g cm^{-1} s^{-2})	Mean (°C)	Variance (°C^2)
(a) *Summary statistics of current meters for the period from 24 April 1998 to 24 April 1999*										
S1	62°48′N	490	100	363	34.4	60	737	126	8.7	0.3
	04°15′E		300	363	34.9	61	730	105	7.8	0.2
			470	298	25.3	60	420	91	6.8	1.8
S2	62°53′N	720	100	365	31.7	61	662	144	8.2	0.3
	04°06′E		300	365	28.6	60	522	103	6.7	1.0
			500	365	13.6	59	184	89	2.0	3.2
			700	365	9.7	62	143	95	−0.8	0.1
SE1	63°00′N	900	100	94	18.7	49	404	224	8.4	0.6
	04°06′E		300	365	12.6	35	190	109	6.9	0.7
			500	365	5.2	39	69	55	1.9	1.4
			880	253	5.3	20	80	65	−0.9	0.0
SE2	63°06′N	1001	100	337	4.5	341	158	147	8.2	0.5
	03°39′E		300	365	3.6	335	100	94	6.6	0.6
			500	365	2.1	253	54	52	1.1	1.0
			880	213	1.2	229	54	53	−1.0	0.0
(b) *Summary statistics of current meters for the period from 8 April 1999 to 8 April 2000*										
S1	62°48′	490	100	365	34.8	59	740	118	8.7	0.5
	04°15′E		300	365	35.5	59	739	93	7.7	0.2
			470	365	28.3	60	511	99	6.7	1.3
S2	62°53′N	720	100	365	33.7	60	736	153	8.5	0.5
	04°06′E		300	365	29.9	62	569	108	7.4	0.6
			500	365	18.0	61	250	82	3.1	3.0
			700	366	9.7	56	128	80	−0.7	0.1
SE1	63°00′N	900	100	366	14.1	42	320	218	8.6	0.7
	04°06′E		300	365	12.3	40	228	151	7.1	0.7
			500	365	7.0	34	104	80	2.8	2.7
			880	366	3.6	48	129	123	−0.8	0.0
SE2	63°06′N	1001	100	365	3.2	349	201	195	8.5	0.8
	03°39′E		300	365	4.0	338	144	136	6.9	0.9
			500	365	3.2	275	87	82	2.0	1.9
			880	281	3.8	213	90	82	−0.9	0.0

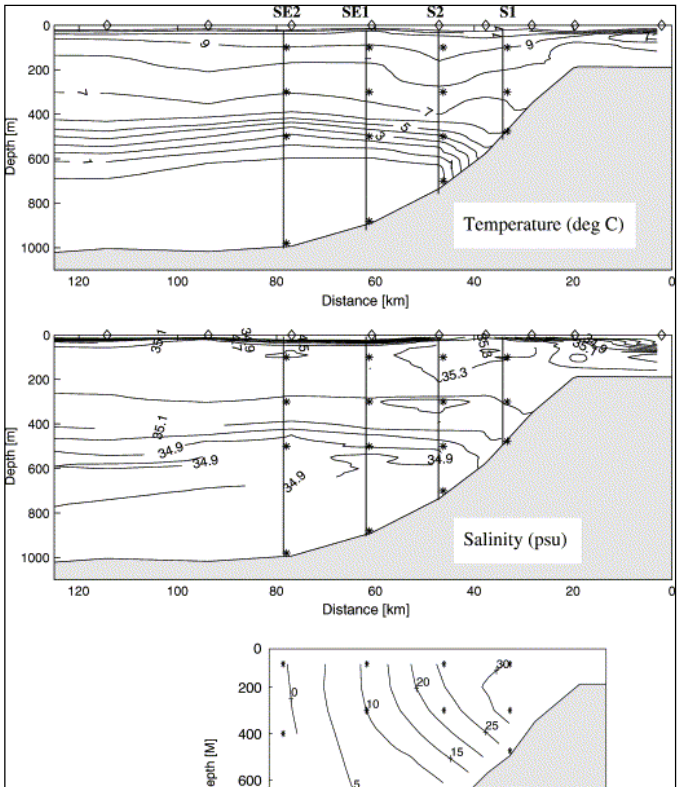

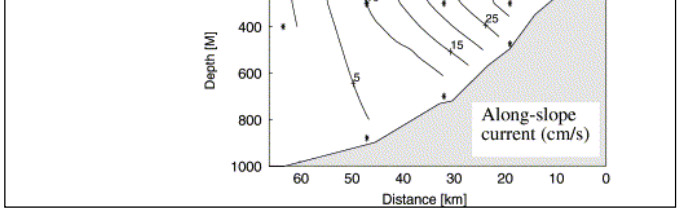

Fig. 2. Temperature and salinity in the eastern part of the Svinøy section (a), and annual along-slope mean current in the region of the continental shelf break (b). Vertical lines show moorings and stars (*) show the location of current meters.

The data analysis is performed by splitting the 2-year time series into two 1-year segments. The segment for the period 1998–1999 is then used for construction of the model, while the 1999–2000 segment is used for testing and validation purposes. The model will be validated by comparison of statistical parameters, including testing of statistical stationarity of the two 1-year segments. The hourly sampled RCM data were processed as follows:

(1) *Data sampling*. A moving average filter with cut off period of 25 h is applied to the original 1-hour RCM-records, and subsequently the records are decimated and resampled as daily samples. The cutoff period of 25 h effectively removes the semidiurnal and diurnal tidal signals, which in any case are relatively small in this area (Orvik et al., 2001). The detided daily samples form the basic data set in this study.

(2) *Data gridding*. Due to data gaps of various lengths (Table 1), it is convenient to grid the data. We use a regular grid with horizontal resolution of 6 km and vertical resolution of 100 m. From the 15 current meter records we obtain gridded fields by using the velocity component normal to the Svinøy section (v) and the temperature (T). The gridding procedure is performed with a bi-harmonic spline method (Sandwell, 1987).

(3) Based on the two gridded fields of current (v) and temperature (T), we calculate total volume transport of AW. The AW is restricted to the water mass with salinity of S>35.0 (Helland-Hansen and Nansen, 1909), corresponding to temperature T>5°C (Orvik et al., 2001).

(4) To identify the optimal current meter location for modeling purposes, we correlate the gridded current field v (normal to the Svinøy section) against the total volume transport for each time series segment; for the model period and the test period, respectively. We apply moving average filters consecutively for [1 (basic data), 3, 7, 30]-day cut off periods. The correlation fields are presented in Fig. 3(a) for the model period and in Fig. 3(b) for the test period.

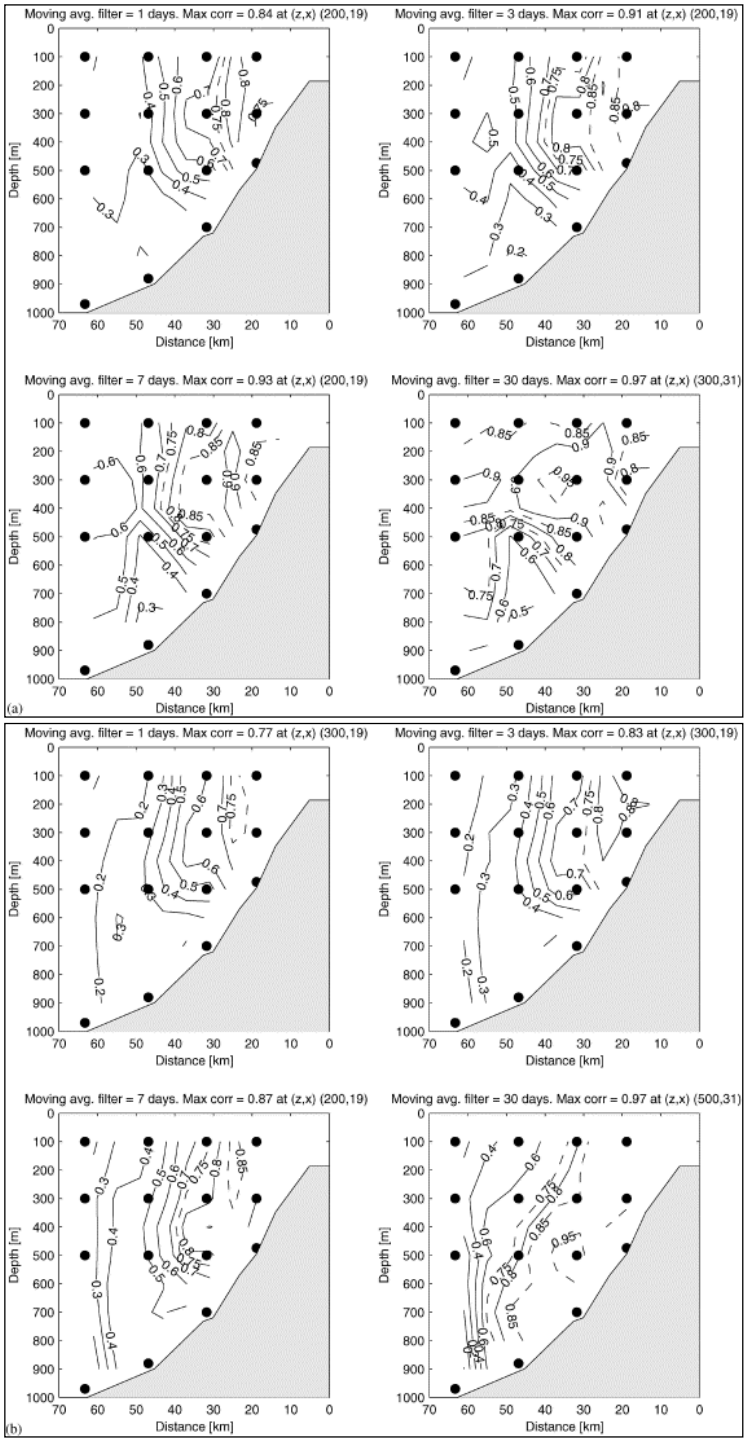

Fig. 3. Correlation fields for calculated volume transport vs. velocity components normal to the Svinøy section (v) in a regular grid with a horizontal resolution of 6 km and vertical resolution of 100 m, constructed

from the 15 RCM records (&z.cirf;) using a bi-harmonic spline method (Sandwell, 1987). The grids obtained using [1, 3, 7, 30]-day moving average filters, respectively, on (a) model period and (b) test period.

(5) For each 7 day filtered current meter record, a linear regression model is constructed in terms of volume transport of AW (V_t) as the dependant variable and current speed v, as the independent variable; $V_t=a_0+a_1v$. Since the most suitable current meters appear to be located in the core of the NwASC (Orvik et al., 2001), it is justifiable to constrain the solution to fit the condition of $V_t=0$ for zero current ($v=0$), yielding the coefficient $a_0=0$. The dependent model parameter V_t is fitted to the independent variable v using a least squares method. Linear regression models are constructed based on all 15 current meter time series, for both the model period and the test period. Calculated coefficients a_1 and correlation coefficients between modeled and calculated transports are presented in Table 2(a) for the model period and in Table 2(b) for the test period.

Table 2. Calculated coefficients a_1 of linear regression model in terms of volume transport $V_t=a_1v$, using each current speed v, as independent variables, and correlation coefficients r between calculated transports and model transport based on each of the 15 RCM records

RCM depth	S1–100	300	470	S2–100	300	500	700	SE1–100	300	500	880	SE2–100	300	500	980
(a) *Model data set. 7-day mov. Average: Y=av*															
Cof *a*	0.13	0.13	0.18	0.14	0.16	0.29	0.40	0.22	0.30	0.47	0.69	0.22	0.24	−0.13	−0.29
Cor, *r*	0.87	0.80	0.80	0.73	0.86	0.75	0.33	0.06	0.54	0.32	0.18	0.47	0.59	0.57	0.32
(b) *Test data set. 7-day mov. Average: Y=av*															
Cof *a*	0.13	0.13	0.16	0.14	0.15	0.24	0.40	0.21	0.25	0.39	0.34	0.12	0.15	−0.18	−0.38
Cor, *r*	0.80	0.79	0.72	0.72	0.77	0.77	0.29	0.35	0.43	0.44	0.18	0.47	0.59	0.57	0.32

(6) A similar coherence analysis for each current time series against volume transport was also performed, and is tabulated for time segments in the [1, 3]-day, [3, 8]-day, and [8, 32]-day time intervals in Table 3. In Fig. 4 the coherence between each current meter record and volume flux vs. frequency is also presented graphically; (a) for the model period and (b) for the test period.

Table 3. Maximum coherence between each of the 15 RCM time series and calculated volume transport tabulated in the $[1^{-1}\text{-}3^{-1}]$-day^{-1}, $[3^{-1}\text{-}8^{-1}]$-day^{-1}, and $[8^{-1}\text{-}32^{-1}]$-day^{-1} frequency bands

RCM Days^{-1}	S1–100	300	470	S2–100	300	500	700	SE1–100	300	500	880	SE2–100	300	500	980
(a) *Model data set. 1-day mov. Average filter*															
$1–3^{-1}$	0.51	0.58	0.26	0.46	0.35	0.39	0.26	0.12	0.06	0.11	0.37	0.16	0.12	0.14	0.16
$3^{-1}–8^{-1}$	0.63	0.69	0.61	0.30	0.43	0.27	0.39	0.10	0.12	0.11	0.50	0.16	0.22	0.21	0.14
$8^{-1}–32^{-1}$	0.86	0.88	0.76	0.43	0.45	0.54	0.10	0.12	0.12	0.08	0.07	0.05	0.02	0.06	0.14
(b) *Test data set. 1-day mov. Average filter*															
$1–3^{-1}$	0.48	0.58	0.40	0.47	0.42	0.43	0.32	0.06	0.09	0.37	0.33	0.18	0.22	0.37	0.39
$3^{-1}–8^{-1}$	0.54	0.57	0.47	0.42	0.35	0.07	0.21	0.34	0.25	0.19	0.19	0.18	0.19	0.37	0.39
$8^{-1}–32^{-1}$	0.72	0.81	0.66	0.53	0.59	0.30	0.12	0.13	0.10	0.07	0.08	0.25	0.24	0.18	0.32

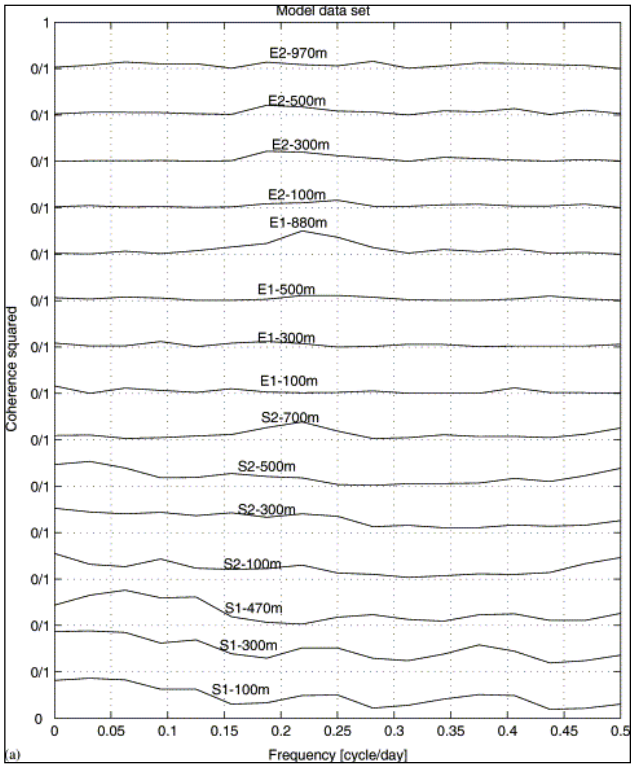

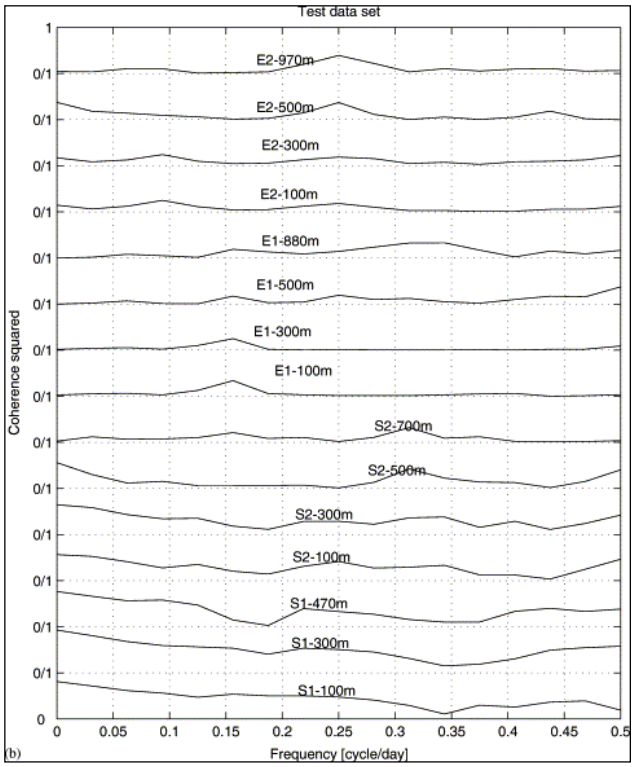

Fig. 4. Coherence between each RCM time series and calculated volume transport vs frequency, based on 1-day average data for (a) model period, (b) test period.

(7) The current meter record S1–100 is used for a supplementary analysis by constructing regression models of estimated volume transport V_t versus current speed (v) in scatter diagrams. The regression lines for the linear model (5) and a non-linear given by a second-degree polynomial as $V_t=a_1v+a_2v^2$, are constructed using [1, 3, 7, 30]-day filtered time series. They are presented with their associated curve and correlation coefficients in Figs. 5a–b.

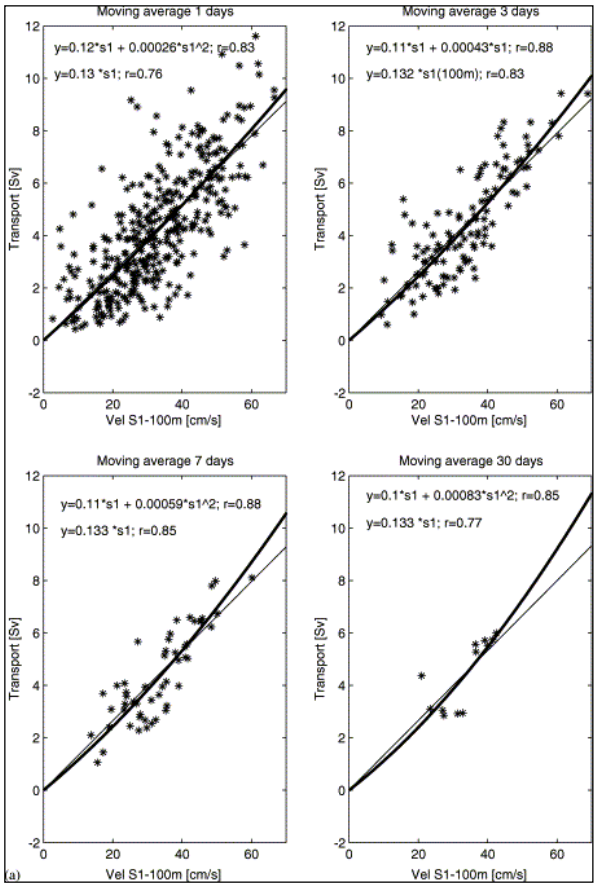

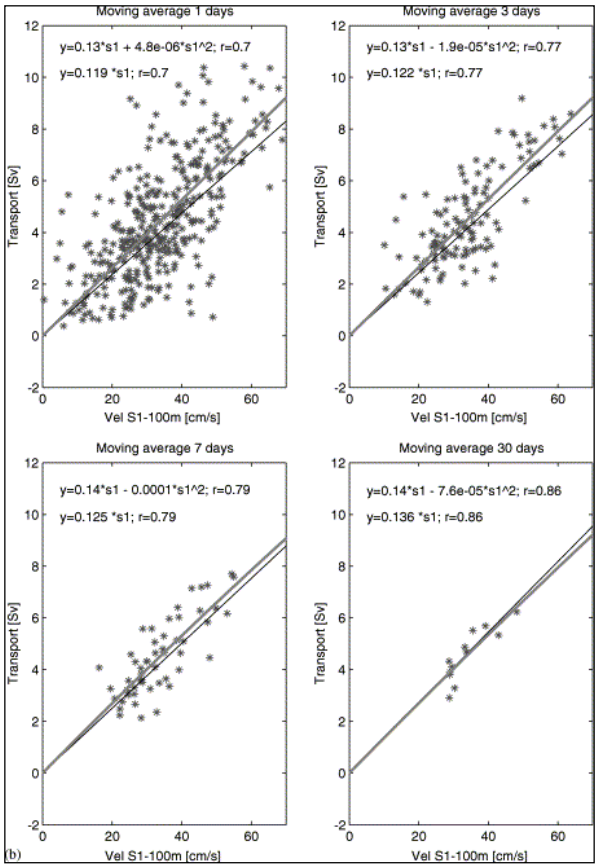

Fig. 5. Scatter plots and linear and non-linear (second-degree polynomial) regression lines from S1–100 m current vs. calculated transport and correlation coefficients, performed for moving average filters of [1, 3, 7, 30]-days; (a) model period (b) test period.

(8) In order to validate the model visually, we present the 2-year time series 1998–2000 for calculated volume transport and model volume transport using the linear regression model S1–100 in Fig. 6, filtered with [1, 7, 30]-day moving averages.

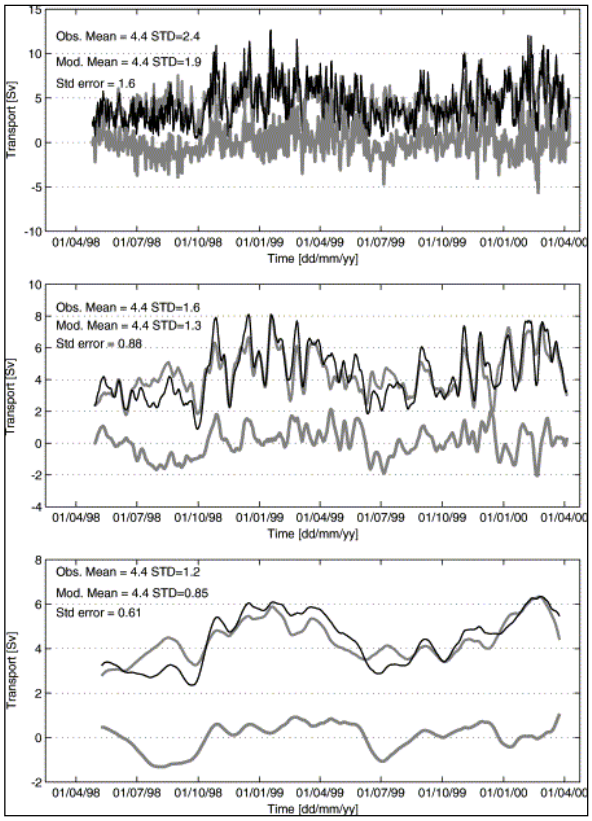

Fig. 6. Two-year time series (1998–2000) of model volume transport from the linear regression model S1–100 as $V_t=a_1 v$ (thick lines), and calculated volume transport (thin lines) and standard error (lower thick lines), using moving average filter of [1, 7, 30]-days. Mean transports and standard deviation for model and calculated transport are shown in each panel, with corresponding correlation coefficients of (0.75, 0.84, 0.86).

3. Results of analysis

3.1. Evaluation

The four-mooring array established in the slope area of the Svinøy section intercepts the NwASC completely and reveals the NwASC as a topographically trapped current, about 40 km wide (Orvik et al., 2001). In order to test the robustness and applicability of the use of a single current meter method for monitoring the NwASC, we have investigated the connection between each current meter record and the volume transport. Then in principle each of the 15 current meter time series should be correlated against the calculated volume transport in order to determine the optimal current meter location for monitoring. For that purpose, we correlate the time series of the gridded current field against the calculated volume transport and present the results in terms of correlation fields. The low pass filtering was performed using moving average filters

with [1, 3, 7, 30]- day cut-off periods on the 1-year model time series and the test time series, respectively. The correlation fields in an *xz*-plane are shown in Fig. 3(a) the model period and Fig. 3(b) the test period.

For the model period the absolute maximum correlation coefficients have an increasing trend, being (0.84, 0.91, 0.93, 0.97) with respect to the [1,3,7,30]-day time scales, while the corresponding results for the test period are (0.77, 0.83, 0.87, 0.97); i.e. there is a lower maximum correlation on shorter timescales but one of same order on the 7-day and 30-day timescales. On the 7-day timescale, Fig. 3 shows maximum values in a band above 0.80 around moorings S1 and S2, extending down to about 500 m depth. The maxima in the correlation fields coincide with the AW for the upper 500 m of the water column (Fig. 2), i.e. they are covered by the current meters at 100, 300 and 500 m depth. The correlation fields also agree with the structure of the NwASC (Skagseth and Orvik, 2002), showing that the core of the AI, and in fact the volume transport, is concentrated over the steeper parts of the slope where moorings S1 and S2 are located. In fact these current meters mirror the volume transport fairly well, and a current meter suitably placed in this maximum correlation area, should in principle be sufficient to represent the volume transport of the NwASC. Though the explained variance from one current meter increases for longer time scales, the maximum correlation is 0.91 and 0.83 down to a 3-day time scale, for the two time segments. Since the correlation fields and current statistics in Table 1, are very similar for the two time segments, they substantiate the stationarity of the current field for these 2 years.

Due to the high correlation field (Fig. 3) in an area over the steepest slope where moorings S1 and S2 are located, both for the model and test data set, we attempt to estimate the volume transport of AW by constructing single linear regression models with volume transport V_t as the dependent variable and current records v as the independent variable, as defined in Section 2. Since the correlation fields show a maximum in the core of the NwASC where mooring S1 is located (Orvik et al., 2001), it is justifiable to constrain the solution to fit the condition V_t=0 for zero current (v=0). Linear regression models are then constructed for all 15 current meter time series, based on 7-day filtered data, and calculated coefficients a_1 and correlation coefficients between model and real transports are presented in Table 2(a) for the model, and in Table 2(b) for the test. Overall, the results in Table 2 coincide with the correlation fields in Fig. 3, and accordingly show maximum correlation coefficients for the current meters on moorings S1 and S2 (except at 700 m depth). For the model period the absolute maximum in correlation is 0.86 for both S1–100 and S2–300, while the corresponding numbers for the test period are 0.80 and 0.77, respectively. For both time segments, the slope coefficients a_1 of the regression lines are calculated to be 0.13 for S1–100/300 and 0.14/0.15 for S2–100/300. In fact, Table 2 shows the best fit and stability for the current meter records S1–100/300, with rather lower confidence for current records on mooring S2.

The corresponding coherence analysis for each current meter record in specific frequency bands (Table 3) shows a maximum for current records S1–100/300 with an average of about 0.75 in the [1–3]-day interval, increasing to 0.80 in the [3–8]-day interval, and 0.93 in the [8, 32] day time interval, for both the model and test periods. The other current records in the core of the AI (e.g. S2–100) show coherence less than about 0.70 for all time intervals, respectively. For the remaining current meter records, Table 3 shows a further decreasing trend. The coherence in Fig. 4, plotted continuously vs. frequency, shows a more detailed, but very similar pattern in accordance with Table 3. For the test period the current records S1–100/300 show an increasing trend for timescales longer than 3 days, while for the model period there are local maxima in the 4–5 day interval and around 2.5 days. The current records S2–100/300 also show an increasing trend, but on a lower level. Indeed, Fig. 4 shows the highest coherence for the current records S1–100 and S1-300. Accordingly, the figure also shows an increasing trend in coherence toward lower frequencies (longer periods) from a 3 day period. In spite of some deviations between the model and test time series, the overall similarity confirms the stationarity of the model, for this particular 2-year period. The increasing trend in coherence toward lower frequencies also agrees with the trend in the correlation fields in Fig. 3.

For both 1-year segments, Table 2 and Table 3 and Fig. 3 and Fig. 4 reveal an overall maximum correlation and coherence between volume transport and each current meter record for S1–100. Accordingly, this current meter turns out to be the optimal choice for a simple regression model for monitoring. Based on that fact, current record S1–100 is used in a supplementary analysis to elucidate its applicability, presented in terms of scatter diagrams of current speed (v) vs. estimated volume transport (V_t) on [1, 3, 7, 30]-day timescales in Fig. 5(a) model and in Fig. 5(b) test period. The regression lines for the linear and non-linear model are constructed according to Section 2. In a broad sense, the scatter plots and linear regression lines agree with the correlation/coherence analysis. The lower correlation coefficients for daily values are reflected in more scattered data, while for longer timescales the higher correlation is exhibited in an alignment of the scatter plots where the data fit the linear regression lines quite well. Indeed, the straight-line fits to the sets of data points have overall slope coefficients of $a_1 \cong 0.13$, in the time range from 1 to 30 days, both for the model and test period. This shows a similar connection between the current records and estimated transport for all time scales investigated. So according to Fig. 5, the regression models for both the model and test period show very similar properties with respect to resolving the volume transport, and support its stability and applicability for these two consecutive 1-year periods. For both the model and test period, the correlation coefficients show a similar trend increasing from about 0.77 on a 7-day timescale to 0.85 on a 30-day timescale; except for the model period on the monthly timescale. The discrepancy in correlation for this particular case is likely to be caused by the limited number of data points. Fig. 5(a) shows that one single point deviates substantially from the regression line. In spite of this particular point off the line, the straight-line fits to the set of data points with a constant slope coefficient of $a_1 \cong 0.13$ on all timescales studied, demonstrating the stability and robustness of the model.

Fig. 5 shows the largest deviations between the linear regression lines and the data points for higher values. This results in an underestimation of larger volume transports, while medium and small volume transports fit the linear regression lines quite well. It is likely that this discrepancy between the regression line and data points for higher transports is a non-linear effect, explained by the widening of the flow for stronger current events (Orvik et al., 2001). This is demonstrated by the non-linear regression line, showing an improvement in fitting the data, partifularly for strong currents. However, the non-linear model shows more variability in its coefficients, indicating a more sensitive and less stable model. With the exception of the particular event in Fig. 5(a), the correlation coefficients show little improvement in terms of increasing correlation coefficients for the non-linear model, when compared with the linear model.

3.2. Application

In order to demonstrate the applicability and confidence of a linear regression model as estimator for the volume flux of the NwASC, the S1–100 regression model is presented as time series in Fig. 6. The correlation coefficients demonstrated in Fig. 5 justify the use of this model on time scales ranging from days to months. In this case, the S1–100 regression model is constructed from the 1-year model data period April 1998–April 1999 (Section 2), and then applied for the 2-year period April 1998–April 2000. The time series are low pass filtered by using moving average filters with [1, 7, 30]-day cutoffs and then presented in Fig. 6. The same procedure is performed on the time series of calculated volume fluxes, also presented in Fig. 6. The model fitness to the real volume flux is shown in terms of correlation coefficients between modeled and calculated volume transport, which are (0.75, 0.84, 0.86) on [1,7,30]-day timescales.

The 2-year time series in Fig. 6 show that the volume transport of the NwASC has fluctuations over a wide range of periods, from a few days to months and seasons, where the seasonal cycle with winter maxima and summer minima appears to be most prominent. The time series show an overall average volume transport of 4.4 Sv, both for the model and real time series on daily to 30-day timescales, illustrating the linearity of the flow. For the real time series the variability in terms of standard deviation is (2.4, 1.6, 1.2)-Sv on [1, 7, 30]-day timescale, while the corresponding numbers for the model are (1.9, 1.3, 0.8)-Sv, respectively. This trend of decreasing standard deviations and differences for the model volume transport compared with the real transport, shows that the model is more sensitive in resolving higher frequency fluctuations. This is also confirmed in a decreasing trend in standard error difference toward longer timescales. This in fact coincides with the weakness of the linear model for high transport, shown in the scatter diagrams in Fig. 5. They clearly show that the linear model underestimates the higher transport values on shorter periods, which is in accordance with the decrease of the correlation coefficients.

The model and real transport time series in combination with the standard deviation errors in Fig. 6, agree with the statistical parameters and correlation analysis. It turns out that the time series are less noisy for longer timescales. The standard deviation error shows a decreasing trend (1.6, 1.3, 0.6)-Sv for [1,7,30]-day timescales, respectively. This is also demonstrated by the curve fitting of the model transport to the real volume transport in Fig. 6. The time series show a noisy pattern for the 1-day timescale, while the curves coincide well both on 7- and 30-day timescales, except for striking events in July–September 1998 and August 1999. This discrepancy, with an error of about 1 Sv on the 30-day timescale, seems to account for most of the standard deviation error. The time series also show that the model underestimates maximum transport events, in accordance with Fig. 5. On a 7-day time scale the underestimates appear to be up to 2 Sv, while they are less than 0.7 Sv on the 30-day timescale, except for the two striking events. So particularly on longer time scales, Fig. 6 reveals that model time series fit the real transport well and coincide within a margin of 0.6 Sv.

4. Discussion and conclusions

The scope of this study is to develop a method to establish a simple, confident and cost effective monitoring system for the AI in the NwASC. In order to achieve this goal, we propose and validate simple regression models, based on a single current meter located in the NwASC. The study is principally based on linear regression models, but is also extended to a non-linear model for testing of potential improvements. In order to validate the statistical stationarity and stability of the models, the 2-year time series 1998–2000 is split into two 1-year segments, a model period and a test period. Similar analyses are then performed on both time segments, for comparison. One-year segments are used in order to weight and resolve the annual cycle properly. The correlation/coherence analysis performed between calculated volume transport and the gridded current field of the NwASC, turned out to be suitable for selecting the optimal current meter location for monitoring. To extend the correlation and coherence analysis, linear regression models for each of the current meter records are constructed, for both the model and the test period. This makes it feasible to test model stationarity by performing similar analyses for the model and test period, and then comparing statistical parameters in combination with the associated coefficients of the regression lines. From this analysis, the current meter records on moorings S1 and S2, turned out to be most suitable for monitoring purposes, with the optimal choice of current meter being S1–100. Further, the correlation and coherence analysis support the inference that moorings S1 and S2 are located in the core of the NwASC, and justify their applicability for use in simple models for monitoring purposes. Indeed, current record S1–100 can be shown to be suitable as a basis for a supplementing analysis by (1) constructing a simple linear regression model, and (2) extending the linear model to a non-linear regression model using a second-degree polynomial.

The scatter plots and regression lines in Fig. 5 show underestimation of the transport for high velocities. This is also demonstrated in the 2-year time series shown in Fig. 6. The underestimation is probably caused by widening of the flow during high speed events, i.e. a non-linear effect (Orvik et al., 2001). In an attempt to improve the linear regression model, we used the second-degree non-linear model mentioned above. According to Fig. 5, the non-linear model shows an improvement in the curve fitting for strong currents, but in general the correlation coefficients show a minor increase compared with the linear model. An apparent weakness with the non-linear model, is less stability in the associated curve coefficients (Fig. 5) over a wider time interval. So in an overall validation, we found the linear regression model to be the most applicable for monitoring the NwASC. The stationarity and stability of the linear regression model are manifested in a constant slope coefficient on all timescales investigated, both for model and test period. Indeed, the robustness, stability and stationarity of the linear regression model are advantageous for the establishment of a monitoring system, as demonstrated in the 2-year time series shown in Fig. 6.

By comparing the real volume transport with transport estimates from the regression model for S1–100 over the time scales ranging from 1 day to 1 month, we see that they all show a fairly similar pattern, except during the periods July–September 1998 and July 1999. These striking events with discrepancies in terms of standard error up to 1 Sv on a monthly timescale, demonstrate the limitation of the simple model in

resolving particular events. Except for these particular periods, the results are convincing with an overall transport of 4.4 Sv both for the model and the real estimates on all timescales. There is also a decreasing trend in standard deviation difference showing the improvement of the model in resolving longer period variability and weakness in fitting shorter period fluctuations. The scatter plot analysis shows that a minor improvement is gained by extending the linear model to a non-linear second-degree polynomial. There are some gains in resolving higher events, but these are nullified by the instability and reduction in confidence of the model coefficients. This substantiates the use of a linear regression model.

This study, as well as earlier studies (Orvik and Mork, 1996, Orvik et al., 2001), has shown that the Svinøy section is very suitable for monitoring the Atlantic inflow to the Nordic Seas. This is in fact because the Svinøy section cuts through both branches of the NwAC; the NwASC and the Polar frontal jet. In this particular study, simple and robust systems for monitoring the Atlantic inflow in the NwASC have been validated. The study has shown that one current meter properly deployed in the core of the NwASC, will capture the gross variability of the flow, and is thus suitable for monitoring purposes. The applicability and confidence of a linear regression model is demonstrated for monitoring the NwASC. These findings disagree with the opinion of McClimans et al. (1999), who stated that high-quality measurements for monitoring purposes, require current meter moorings spaced at distances as fine as 3 km, which would be prohibitively expensive.

Acknowledgements

This study is a contribution to the Svinøy section monitoring program, which was initiated in 1995 and is still in progress. The program was funded initially by the Norwegian Research Council and again from year 2000. For the period 1997 to 2000 the program has been run as a part of the EU-MAST-funded Variability of Exchanges In the Northern Seas (VEINS) program. Thanks are also due to support from the Norwegian Deepwater Program (NDP), making continuation of the program possible, and to Alastair Jenkins reviewing the manuscript.

References

Helland-Hansen and Nansen (1909). Helland-Hansen, B., Nansen, F., 1909. The Norwegian Sea: its Physical Oceanography based upon Norwegian Research 1900–1904, Part 1, No. 2. Fiskeridirektorates Skrifter, Serie Havundersoekelser 3, 390.

Johannessen et al (1999). O.M. Johannessen, E.V. Shalina and M.W. Miles , Satellite evidence for an arctic sea ice cover in transformation. *Science* **286** (1999), pp. 1937–1939.

McClimans et al (1999). T. McClimans, B.O. Johannessen and T. Jenserud , Monitoring a shelf edge current using bottom pressures or coastal sea-level data. *Continental Shelf Research* **19** (1999), pp. 1265–1283.

Mosby (1970). H. Mosby , Atlantic water in the Norwegian Sea. *Geophys. Norv.* **28** 1 (1970), p. 60pp.

Orvik and Mork (1996). Orvik, K.A., Mork, M., 1996. Atlantic water transport from long-term current measurements in the Svinøy section. ICES CM 1996/O: 8, 9pp.

Orvik and Niiler (2002). K.A. Orvik and P. Niiler , Major pathways of Atlantic water in the northern North Atlantic and Nordic Seas toward Arctic. *Geophysical Research Letters* **29** 19 (2002), pp. 1896–1899.

Orvik et al (2001). K.A. Orvik, Ø. Skagseth and M. Mork , Atlantic inflow to the Nordic Seas. Current structure and volume fluxes from moored current meters VM-ADCP and Seasoar-CTD observations 1995–1999. *Deep-Sea Research I* **48** 4 (2001), pp. 937–957.

Pistek and Johnson (1992). P. Pistek and D.R. Johnson , Transport of the Norwegian Atlantic Current as determined from satellite altimetry. *Geophysical Research Letters* **10** 13 (1992), pp. 1379–1382.

Poulain et al (1996). P.-M. Poulain, A. Warn-Varnas and P.P. Niiler , Near-surface circulation of the Nordic seas as measured by Lagrangian drifters. *Journal of Geophysical Research* **101** C8 (1996), pp. 18237–18258.

Rahmstorf (1999). S. Rahmstorf , Shifting seas in the greenhouse. *Nature* **399** (1999), pp. 523–524.

Rothrock et al (1999). D.A. Rothrock, Y. Yu and G.A. Maykut , Thinning of Arctic sea ice cover. *Geophysical Research Letters* **26** (1999), pp. 3469–3472.

Samuel et al (1994). Samuel, P., Johannessen, J.A., Johannessen, O.M., 1994. A Study on the Inflow of Atlantic Water to the GIN Sea using GEOSAT Altimeter Data. In: Johannessen, O.M., Muench, R.D., Overland, J.E. (Eds.), The Polar Ocean and their Role in Shaping the Global Environment: The Nansen Centennial Volume. AGU Geophysical Monograph 85, 95–108.

Sandwell (1987). D.T. Sandwell , Biharmonic spline interpolation of GEOS-3 and SEASAT altimeter data. *Geophysical Research Letters* **14** (1987), pp. 139–142.

Skagseth and Orvik (2002). Ø. Skagseth and K.A. Orvik , Identifying fluctuations in the Norwegian Atlantic Slope Current by means of empirical orthogonal functions. *Continental Shelf Research* **22** (2002), pp. 547–563.

Tait (1957). J.B. Tait , Hydrography of the Faroe–Shetland Channel 1927–1952. *Marine Research (Edinburgh)* **2** (1957), pp. 1–309.

Wood et al (1999). R.A. Wood, A.B. Keen, F.B. Mitchell and J.M. Gregory , Changing spatial structure of the thermohaline circulation in response to atmospheric CO_2 forcing in a climate model. *Nature* **399** (1999), pp. 572–575.

Worthington (1970). L.V. Worthington , The Norwegian Sea as a Mediterranean basin. *Deep-Sea Research I* **17** (1970), pp. 77–84.